BIOCHEMISTRY
including biophysical chemistry & molecular biology

ARTICLE

pubs.acs.org/biochemistry

Aspartate 102 in the Heme Domain of Soluble Guanylyl Cyclase Has a Key Role in NO Activation

Padmamalini Baskaran,[†] Erin J. Heckler,[†] Focco van den Akker,[*,‡] and Annie Beuve[*,†]

[†]Department of Pharmacology and Physiology, New Jersey Medical School, UMDNJ, Newark, New Jersey 07103, United States

[‡]Department of Biochemistry, Case Western Reserve University, Cleveland, Ohio 44120, United States

Supporting Information

ABSTRACT: Nitric oxide (NO) is involved in the physiology and pathophysiology of the cardiovascular and neuronal systems via activation of soluble guanylyl cyclase (sGC), a heme-containing heterodimer. Recent structural studies have allowed a better understanding of the residues that dictate the affinity and binding of NO to the heme and the resulting breakage of the bond between the heme iron and histidine 105 (H105) of the β subunit of sGC. Still, it is unknown how the breakage of the iron−His bond translates into NO-dependent increased catalysis. Structural studies on homologous H-NOX domains in various states pointed to a role for movement of the H105 containing αF helix. Our modeling of the heme-binding domain highlighted conserved residues in the vicinity of H105 that could potentially regulate the extent to which the αF helix shifts and/or propagate the activation signal once the covalent bond with H105 has been broken. These include a direct interaction of αF helix residue aspartate 102 (D102) with the backbone nitrogen of F120. Mutational analysis of this region points to an essential role of the interactions in the vicinity of H105 for heme stability and identifies D102 as having a key role in NO activation following breakage of the iron−His bond.

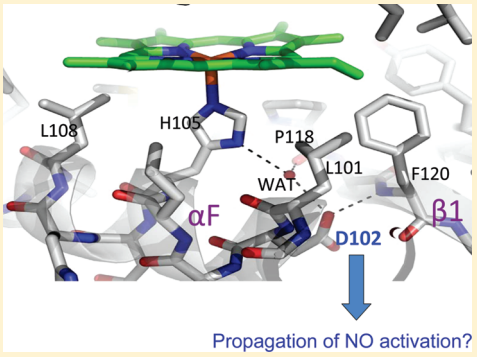

Soluble guanylyl cyclase (sGC), a heme-containing heterodimeric enzyme, is the main receptor for nitric oxide (NO). Binding of NO to the heme of sGC increases the production of cGMP several hundred fold. The NO-cGMP pathway is involved in many physiological processes including cardiovascular homeostasis,[1] inhibition of platelet aggregation,[2] and synaptic plasticity.[3] The heme is ligated to His 105 of the β subunit of sGC.[4] Binding of NO to the heme induces the breakage of the heme iron−His bond leading to increased catalysis. We and others have solved structures of prokaryotic analogue heme domains (HNOX) in the presence of various ligands, allowing a better understanding of the initial events in NO-dependent stimulation of sGC,[5−7] in addition to molecular dynamic simulation.[8] Mutational analyses have in turn identified residues critical for the heme stability and binding.[9,10] Furthermore, potential inhibitory interactions between the heme domain and the catalytic domain that would be released upon binding of NO were suggested as a mechanism of activation.[11,12] In spite of all these studies, the major challenge remains to understand the mechanism of propagation of the NO signal, in particular, the conformational events following breakage of the iron−His bond. Through comparison between the inactive and active structures of the HNOX domains,[13,14] we anticipate that one region undergoes major shift upon binding of NO, the αF helix.[7] Our homology modeling showed that His 105 (H105), being liganded to the heme in the inactive state, is surrounded by residues conserved in both *Nostoc* H-NOX and sGC β1 heme domain pointing to a potentially critical role. These conserved residues include D102 which is the only other αF helix residue that is predicted to make a direct hydrogen-bonding interaction with the backbone nitrogen of phenylalanine 120 (F120) belonging to the β1 strand (Figure 1). Since the postulated shifting αF helix is only held in place to the rest of the H-NOX domain via the NO-labile H105−Fe bond and the D102/F120 interactions (in addition to other van der Waals interactions involving the αF helix), we investigated the activation importance of these residues. Furthermore, residues D102 and H105 are also in contact via a water-mediated interaction in the *Nostoc* structure that was also present in the sGC homology model. This water molecule likely provides bridging interactions with the backbone oxygen of P118, also a key conserved β1-strand residue found to be important for H-NOX function.[15] We therefore speculate that these conserved interactions between the αF helix and β1 strand residues in the vicinity of H105 could be relaying key NO-dependent conformational activation changes. Residue D102 is partially solvent exposed as only one of its oxygens is involved in hydrogen bonding to F120, thereby offering the possibility that D102 is potentially involved in communicating conformational changes to other domains of sGC. Therefore, using structure-based mutational analysis combined with kinetics and spectral

Received: December 14, 2010
Revised: April 12, 2011
Published: April 14, 2011

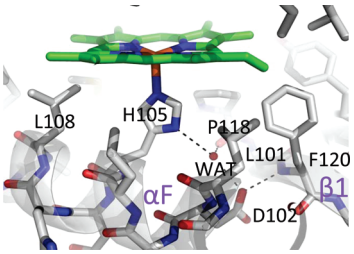

Figure 1. Close-up view of proximal face of the heme in the homology model of the rat sGC β1 H-NOX domain. The helix αF and strand β1 (purple font) are labeled accordingly. The interaction network involving αF helix and β1 strand residues D102, H105, F120, and P118 are shown, including the direct and water-mediated hydrogen bonds (dashed lines). The heme moiety is shown in green.

analysis of the full-length rat sGC, we tested the hypothesis that D102 and other residues in the vicinity are involved in the mechanism of NO propagation from the heme domain to the effector cyclase domain.

EXPERIMENTAL PROCEDURES

Molecular Modeling. A homology model of the rat sGC H-NOX was generated using SWISS-MODEL[16] with the Nostoc H-NOX as the structural template (ref 7; PDB ID: 2O09). After modeling the protein, the position of the heme and water molecule near H105 and D102 were obtained after superpositioning the heme and water containing Nostoc H-NOX crystal structure and the rat sGC β1 H-NOX homology model. Molecular figures were generated using PYMOL.

Reagents. [α-^{32}P]-GTP is from PerkinElmer (Waltham, MA). DMEM is from ATCC (Manassas, VA) and antibiotic/antimycotic from Mediatech, Inc. (Richmond, VA). The expressfect transfection reagent is from Denville Scientific Inc. (Metuchen, NJ) and SF900II SFM medium, FBS, and Gentamycin are from Invitrogen. SNAP is from EMD Chemicals (Gibbstown, NJ) and DEA-NO from Axxora LLC (San Diego, CA). β sGC antibody was purchased from Cayman Chemicals (Ann Arbor, MI). 7.5% Tris-HCl gels are from Bio-Rad Laboratories (Hercules, CA). All the other reagents, including α sGC antibody, were from Sigma.

Mutagenesis of Rat sGC and Transfection in COS-7 Cells. α1 and β1 subunits of rat cDNA subcloned in pCMV5 vector[17] were mutated using Quikchange Site-Directed Mutagenesis Kit (Agilent Technologies, Santa Clara, CA) and confirmed by sequencing. α1 and β1 cDNA wild type (WT) and mutants were transiently transfected in COS-7 cells grown in DMEM supplemented with 10% fetal bovine serum (FBS) and 1% antibiotic/antimycotic (penicillin (100 IU/mL), streptomycin (100 μg/mL), and Amphotericin B (0.25 μg/mL)).

Cytosol Preparation and Western Blot Analysis. After 48 h, transfected COS-7 cells were washed in cold phosphate buffered saline (PBS) and scraped in homogenization buffer (50 mM HEPES, pH 8.0, 150 mM NaCl, 1 mM DTT, protease inhibitors). Cytosol was prepared by sonication and centrifugation at 14 000 rpm for 10 min at 4 °C to remove the membrane fraction and cell debris. Expression level of sGC WT and mutants were assayed by immunoblotting with anti α and anti β antibodies after electrophoresis of 8 to 10 μg of cytosolic protein on a 7.5% Tris-HCl gel.

Construction of Mutant Baculoviruses. Mutations were introduced in the β1 subunit containing an His-tag at the COOH terminus and cloned in the baculovirus transfer vector pBacPAK8 as described previously.[18] Recombinant baculovirus were produced in Sf21 cells by contransfecting plasmid DNA and linear BacPak6 viral DNA as per the manufacturer's protocol (Clontech, Mountain View, CA). The initial virus stock was obtained by collecting the culture supernatants. Virus stocks with high titer were obtained from 50 mL Sf21 suspension culture after 72 h of infection.

Production of Recombinant Protein in Sf21 Cells. Sf21 cells were initially seeded in 2 L of SF900II SFM medium containing gentamycin (0.1 mg/mL) and 5% heat inactivated FBS at 0.5×10^6 cells/mL at 28 °C with constant shaking. Twenty-four hours after seeding (cell density is 1×10^6 cells/mL), cells were coinfected with α1- and β1-His$_{tag}$ WT or mutant containing viruses and grown for 48 h. The cells were pelleted by centrifugation at 1500*g* for 10 min, and the pellet was resuspended in Puck's saline G buffer (1.1 mM Na_2HPO_4, 1.1 mM KH_2PO_4, 137 mM NaCl, 5.4 mM KCl, protease inhibitors). The recombinant protein was purified in two steps: first through a cobalt column (Clontech, Mountain View, CA) and second by FPLC using a Mono Q anion exchange column (GE Health Care, Piscataway, NJ) with an NaCl gradient, as previously described.[18] The elution pattern at 431, 280, and 393 nm was recorded using the Unicorn program of the GE ÄKTA HPLC/FPLC purifier as described in the text. The fractions, which showed a peak at 431 nm (or 280 nm for apo form of sGC mutants), were collected and snap frozen in 10% glycerol and stored at −80 °C.

sGC Activity Assay. sGC activity was measured by the conversion of [α-^{32}P]cGMP from [α-^{32}P]GTP in a reaction mix containing 50 mM HEPES, pH 8.0, 5 mM $MgCl_2$, 500 μM GTP, and 1 mM DTT at 33 °C for 5 min. Typically, 50 μg of COS-7 cytosol transfected with either WT or mutants and 30−100 ng of purified enzyme were used to measure basal, PPIX, YC-1 stimulated activity and DEA-NO, or YC-1 + DEA-NO stimulation. YC-1 stock solution was prepared in DMSO; DMSO concentration in the reaction mixture did not exceed 0.2%. For the screening in COS-7 cells, the NO-donor SNAP was used (longer half-life) but then we switched to DEA-NO for the spectrum and activities analysis of purified preparations as it is an "authentic NO-donor" (SNAP is a nitrosothiol). For concentration−response curves, specific activities were measured at seven different concentrations of DEA-NO ranging from 0.1 to 100 μM and in the absence or presence of 10 μM YC-1 to assess the synergistic effect.

UV/vis Absorption Spectroscopic Analysis. The absorbance spectrum was recorded from 350 to 450 nm using a Shimadzu UV-2450 spectrophotometer for WT and mutants. 100 μL (~0.01 mg/mL) of the sample was scanned in the absence or presence of NO. DEA-NO was used as an NO-donor at a concentration of 10 μM. The level of purification was directly estimated by the ratio OD 431 nm/OD 280 nm simultaneously measured (similar background noise) by the GE ÄKTA FPLC UV-900 detector (equipped with a quartz 4 mm flow cell with titanium housing; monochromator light source is a xenon lamp with two photodiodes, double-beam). Each enzyme was purified two (mutants) to five (WT) times.

Statistical Analysis. The results are expressed as mean ± SEM from the data derived from the [α-^{32}P]GTP assay. For sGC assay in COS-7 cells each experiment was repeated three times, each in duplicate and from two to three independent transfections. For spectral analysis, two to four independently purified enzymes were used. For purified-enzyme assays, two to three

Table 1. Basal and Stimulated Activities of Wild-Type (WT) and HNOX Mutants Transfected in COS-7 Cells[a]

	basal		PPIX, 100 μM		YC-1, 100 μM		SNAP 100 μM		SNAP, 100 μM + YC-1, 100 μM	
	spec act	% of WT	spec act	fold stimul	spec act	fold stimul	spec act	fold stimul	spec act	fold stimul
WT	229 ± 7	100	431 ± 42	1.9	1430 ± 63	6	3328 ± 102	14.5	3402 ± 370	15
D102A	161 ± 21	70	160 ± 5	1	232 ± 26	1.4	354 ± 38	2.2	662 ± 129	4
D102N	47 ± 6	20.5	87 ± 14	1.85	202 ± 28	4	229 ± 17	4.9	1063 ± 77	**22**
D102E	73 ± 17	32	168 ± 20	2.4	128 ± 13	1.7	152 ± 82	2	292 ± 78	4
F120A	169 ± 53	73	108 ± 44	0.64	172 ± 22	1	278 ± 113	1.6	231 ± 28	1.4

[a] Specific activity (spec act) is expressed in pmol min^{-1} mg^{-1} of extracted protein ± SEM and is the result of three independent transfections; for each transfection, the assay was repeated three times (and in duplicate) under each condition. Fold stimulation (fold stimul.) strongly lower or higher than WT is underlined and in bold, respectively. The NO-stimulated values with SNAP were confirmed using DEA-NO (not shown). DEA-NO was then used with purified sGC.

independently purified enzymes were used and assayed three times under each condition and in duplicate. Student's *t* test was used for statistical comparison between groups and conditions with Sigmaplot version 11.0 software (Systat software, San Jose, CA). $P < 0.05$ was considered statistically significant.

RESULTS

Homology Modeling of the Heme Domain of the β1 Subunit (HNOX) Predicts the Presence of a Cavity in the Heme Domain. The recently solved structure of the HNOX domain of *Nostoc* specie (*Ns* H-NOX), which shares 33% homology with the same domain in sGC, was used for homology modeling.[7] Homology modeling of the sGCβ1 H-NOX revealed the conservation of interactions between the αF helix and β1 strand that are also present in the *Nostoc* H-NOX crystal structure. These interactions include the hydrogen bond between D102 and backbone nitrogen of F120 as well as water-mediated interactions between D102, H105, and the backbone oxygen of P118 (Figure 1). These residues are all conserved in *Nostoc* H-NOX and are in the vicinity of H105, suggesting an important role with perhaps the partially solvent exposed D102 residue as a intersubdomain communicator residue. Our hypothesis is that this region provides crucial bridging interactions between the β1 strand and αF helix. In addition, we speculate that, since H105 in the αF helix is anticipated to move upon iron−His bond cleavage, the H105−water−D102 network might shift as well, which could be important for the activation process in full-length sGC. The importance of this region is further strengthened by the absolute conservation of D102 although only one of its oxygen atoms is involved in H-NOX domain interactions, leaving the second, solvent exposed oxygen free for possibly transmitting the NO activation signal. The significance of this region for propagation of NO activation was tested by mutational analysis of the residues near H105 in the αF helix.

Alanine Scanning of Residues Predicted To Be Involved in Propagation of NO Activation. Residues D102 and F120 were replaced with alanine (A) by site directed mutagenesis; in addition, D102 was replaced with asparagine (N) a polar uncharged residue and with glutamate (E) a polar negatively charged residue. cDNA of the WT α subunit was cotransfected with cDNAs of WT or mutants of the β subunit in COS-7 cells. Cytosolic fractions were prepared and activity measured under basal (unstimulated) condition and in the presence of 100 μM protoporphyrin IX (PPIX, an iron free heme activator that activates heme-depleted sGC), 100 μM of YC-1 (a non NO-donor activator), 100 μM of the NO-donor SNAP, or 100 μM of YC-1 and SNAP. Table 1 summarizes the basal or stimulated activity of WT and mutant enzymes transiently expressed in COS-7 cells. The levels of expression were similar for WT and mutants (Figure 1 of Supporting Information).

Replacement of D102 with three different residues (A, N, or E) led to different patterns of activity: basal activity was more affected by replacement with a polar residue (N or E) than in D102A. PPIX activates the WT by 2-fold, and this activation was retained by D102N and D102E but lost in D102A. On the other hand, only D102N was stimulated by YC-1 but to a lower level than WT. The same was true for stimulation with a NO-donor, though the activation of D102N was marginal (4-fold vs 14.5 for the WT). However, activation of D102N with YC-1 and SNAP was intriguingly high, higher than the WT (22-fold vs 15-fold) while weak activation by combined YC-1 and SNAP was seen with D102A and D102E. On the other hand, the mutant F120A retained basal activity but was unable to respond to PPIX, NO or YC-1 and to YC-1 + SNAP. All together, this indicates that this heme region is critical for basal activity (D102N and D102E), for YC-1 activation (D102A, D102E, and F120A), and, less surprisingly, for NO stimulation. PPIX activation was weak even for the WT for two potential reasons: (a) heme is still stable and tightly bound in WT and mutants, or (b) the effect of PPIX is difficult to assess in broken cell preparation. It is important to note that these residues, even though they affect basal catalysis, are located in the heme domain and that their replacement does not affect stability and expression of α and β subunits (Supporting Information Figure 1). To characterize the mechanisms of propagation of NO activation, mutants D102A, D102N, and F120A were purified for spectral and kinetics analyses.

Purification of WT and Mutants. Mutants and WT were expressed with an Sf21/baculovirus system and purified by using a cobalt affinity column (the WT or mutated β subunit carries a COOH-terminal His-tag) followed by FPLC with salt-gradient elution (see Experimental Procedures). As shown in Figure 2A, elution of sGC is detected by monitoring absorbance at 431 nm (nonstimulated heme-containing sGC). The elution profile at 431 nm of the mutants indicated that D102 when replaced with Ala (D102A) led to an apo form of sGC but when replaced with Asn (D102N) retained the heme, suggesting that the presence of a polar residue at this position could be involved in heme stability/affinity. On the other hand, replacement of the bulky F120 with Ala resulted in the loss of the heme, probably indicative of destabilization of interactions in this heme region. For the heme-depleted mutants, the fractions with the highest

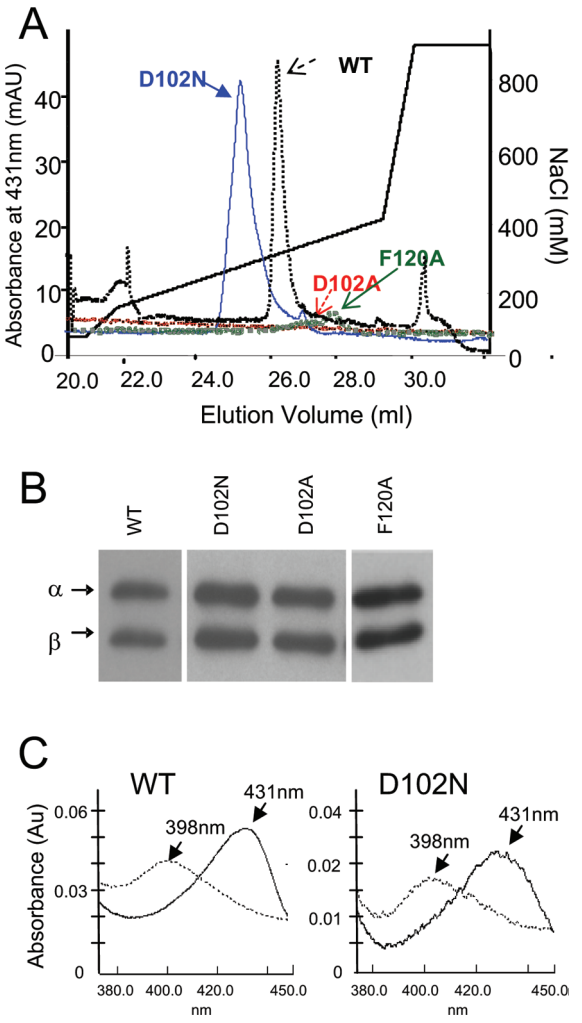

Figure 2. Purification of wild type (WT) and mutants. (A) Representative purification of WT $\alpha1/\beta1$ (black, dashed line) and mutants $\alpha1/\beta1$D102N (blue), $\alpha1/\beta1$D102A (red), and $\alpha1/\beta1$F120A (green). Absorbance at 431 nm (heme containing-enzyme) was monitored with the UV900 detector of the FPLC. WT and mutants elute between 250 and 280 mM NaCl (salt gradient is indicated by a black line). Protein concentration (A280 nm) and oxidation of the heme (A393 nm) were monitored as well (Figure 2 of Supporting Information). (B) WT and mutants had similar levels of expression in the Sf21/baculovirus system as indicated by Western blot with anti-sGC antibodies. (C) UV/vis absorbance of WT and D102N mutant in the absence and presence of 10 μM DEA-NO. Upon addition of DEA-NO similar shift from 431 nm (black line) to 398 nm (dotted line) was observed for WT and D102N mutant.

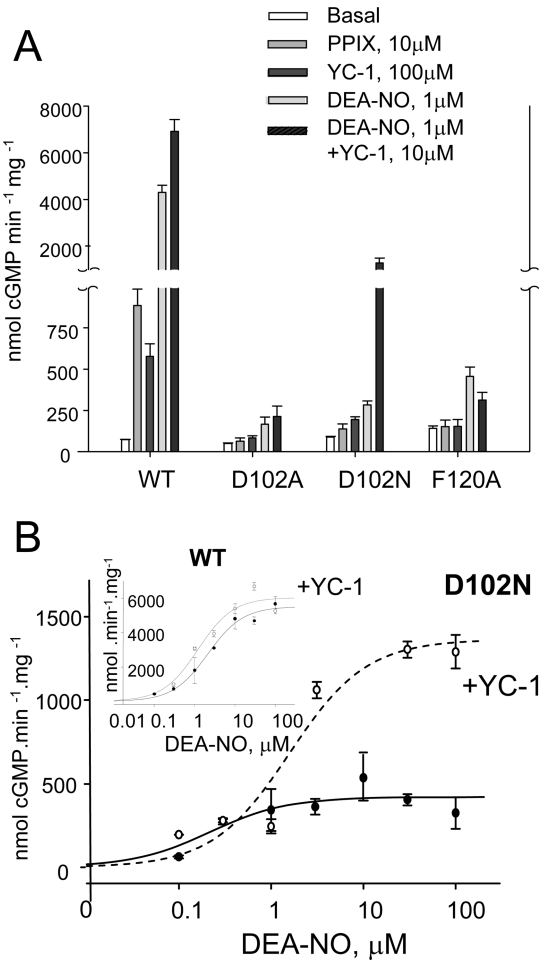

Figure 3. Specific activities and concentration−response curve to NO/YC-1 of purified WT and mutant D102N. (A) Heme mutants lost most of their response to PPIX, YC-1 or DEA-NO but $\alpha1/\beta1$D102N was significantly stimulated by YC-1 + DEA-NO. Measurements of activities were done at least three times on two to three independently purified WT and mutants with each assay done in duplicate under each condition. Results are expressed in nmol cGMP mg^{-1} min^{-1} ± SEM. $P < 0.05$ was considered significant. Values and fold stimulation are provided in Table 2 of Supporting Information. (B) Concentration−response curve to DEA-NO of mutant D012N and WT (inset) in the absence (●) or presence (dashed line, ○) of 10 μM YC-1. Results are expressed in nmol cGMP mg^{-1} min^{-1} ± SD.

280 nm absorbance in the 250−280 mM NaCl elution range were collected and analyzed. Western blot analysis (Figure 2B) showed that for WT and purified mutants both subunits were equally expressed, reflecting a stable heterodimer. The heme depletion in F120A and D102A was confirmed by spectrum analysis of the purified mutants from 350 to 450 nm (not shown). The complete elution profile with monitoring absorbance at 280, 431, and 393 nm (oxidized heme) are depicted in Figure 2 of the Supporting Information. Levels of purification for WT and mutants were estimated by the ratio of protein (280 nm) to heme bound protein (431 nm) (Table 2 of Supporting Information) and by Coomassie staining of the purified WT and mutants (Figure 3 of Supporting Information). The characteristics of purification of WT and mutant D102N were similar. In addition, spectrum analysis for the WT and mutant D012N (Figure 2C) showed a similar shift in the Soret band from 431 to 398 nm upon addition of 10 μM DEA-NO. Formation of the nitrosyl-heme in WT and D102N (NO-activated 5-coordinate form) indicates that the cleavage of H105−iron bond still occurs.

Purified WT and Mutants Basal and Stimulated Specific Activities. Purified WT responded to 10 μM PPIX (12-fold stimulation), 100 μM YC-1 (7.9 fold-stimulation), 1 μM DEA-NO (59.0-fold stimulation), and 10 μM YC-1 + 1 μM DEA-NO (89.8-fold), compared to basal activity (Figure 3A and Table 3 of Supporting Information). D102A and F120A, which were depleted for the heme lost their response to NO stimulation, as expected. However, they also were unresponsive to PPIX as well as YC-1, suggesting that these residues are not only involved in

stability of the heme but probably in the integrity of the heme pocket (as PPIX could not activate these mutants) or in the transmission of the YC-1 and PPIX activation to the catalytic domain. It is not known whether these mutations impaired the binding *per se* of PPIX or YC-1 or their activating effects. Similarly, the response of D102N to PPIX, YC-1 and to DEA-NO was negligible (Figure 3A and Table 3 of Supporting Information), even though D102N retains the heme. Interestingly, mutant D102N remains responsive to the combined stimulation of YC-1 and DEA-NO indicating that NO and YC-1 are still able to interact with the mutant. D102N basal activity was higher in its purified form than in COS-7 cells extracts (for reasons that are unknown), but it could explain why fold stimulation by DEA-NO + YC-1 of the purified form is not as high as in COS-7 cells (as it is a function of the basal activity). The other explanation is that the mutant is less responsive to NO + YC-1, which are used at a lesser concentration in the purified system compared to the COS-7 system (Table 1). Nonetheless, the increase in the mutant activity with the NO and YC-1 combination indicates that both NO and YC-1 bind to the mutant D102N and that the propagation of the NO activation signal is disrupted by the mutation despite the apparent breakage of the His−iron bond (as seen in shift of the Soret band to 398 nm).

DEA-NO Concentration−Response Curves of Purified WT and D102N in the Absence or Presence of YC-1. To investigate the apparent discrepancy between the formation of the heme-nitrosyl 5-coordinate activated form and the very low NO activation but substantial YC-1 + NO activation in D102N, we measured the activity as a function of increasing concentrations of DEA-NO with and without 10 μM YC-1 (Figure 3B). Interestingly, the specific activity of D102N in response to DEA-NO had a maximum at 1 μM and did not increase even at 100 μM, suggesting that the NO-dependent increase in catalytic activity was independent of the amount of NO provided. In other words, the affinity was not impaired in this mutant (as it responded to lower concentration of NO, V_{max} = 0.4 μmol min^{-1} mg^{-1}). Moreover, in the presence of YC-1 at 10 μM, the specific activities were strongly increased at apparent saturating concentrations of NO (3 to 100 μM, V_{max} = 1.3 μmol min^{-1} mg^{-1}). This means that YC-1 did not increase NO-stimulated activity by increasing NO affinity because at NO saturating concentrations, all heme molecules are likely occupied by NO (in fact, the apparent EC_{50} even increases in the presence of YC-1, 1.9 μM vs 0.3 μM with NO alone). In sharp contrast, the WT (inset Figure 3B) had an expected response to increasing concentration of DEA-NO with a V_{max} of ∼5.5 μmol min^{-1} mg^{-1} and an EC_{50} of 2.1 μM while in the presence of YC-1 the response curve shifted left with a lower EC_{50} (1.2 μM) and a small increase in V_{max} (6.2 μmol min^{-1} mg^{-1}). These results showed that in D102N, YC-1 potentiates NO activation not via increased NO affinity but via increased NO efficacy. The potential mechanisms involved are discussed below.

DISCUSSION

Multiple laboratories are engaged in an effort to understand the propagation of the NO signal from the heme-binding domain of sGC to its effector catalytic domain. The reason for such effort is due to the physiological relevance of the NO-cGMP pathway and also to the complexity of sGC as a heme-containing heterodimeric protein, which harbors both functions of receptor and enzyme. It is accepted that breaking of the His−iron heme bond upon binding of NO is a key step in inducing conformational changes leading to increased catalysis in the cyclase domain.[19] What takes place downstream of the His−iron cleavage and how it leads to increased catalytic activity is largely unresolved. To address this fundamental question, we first conducted structural modeling that revealed conserved interactions between the αF helix and β1 strand regions involving H105, D102, and F120. We hypothesized that those interactions could aid or steer αF helix movement upon release of the His−iron heme bond and participate in propagation of NO activation. Replacement of D102 with Ala drastically affects the heme stability or affinity as the mutation led to an apo form of the enzyme, which also failed to respond to PPIX activation, suggesting that this mutation disrupts the propagation of the PPIX activation signal or does not allow PPIX binding. Impaired YC-1 activation in D102A was also observed and could be explained by the inability of YC-1 to bind to the mutant or because YC-1 binds to but does not activate heme-depleted sGC, as previously shown.[20] On the basis of our homology modeling (Figure 1), introduction of an Ala instead of Asp should preclude the predicted interactions with the backbone nitrogen of F120 and the water molecule thus destabilizing interactions in this heme region. Similarly, replacement in this region of F120 with Ala resulted in an apo form of sGC with no activation by PPIX, YC-1, or DEA-NO, underlying the importance of this residue in the stability or affinity of the heme and activation of sGC. The fact that PPIX does not activate this mutant has two possible explanations; the propagation of activation is blocked or PPIX no longer binds to the heme domain. This region also includes P118, whose structural analysis of replacement with Ala (P115A in *Thermoanaerobacter* HNOX) suggested that heme distortion is associated with a large N-terminal shift of the heme domain,[21] leading us to speculate that F120 might have a similar role.

In sharp contrast with the introduction of Ala residues in this region of interactions, replacement of D102 with Asn generates a mutant (D102N) that retains heme. NO still binds to the heme of D102N as it leads to a shift in the Soret band to 398 nm, indicative of His−iron heme breakage. However, the resulting 5-coordinate "activated" form only leads to marginal NO activation. Thus, in this mutant, breakage of the His−iron bond and NO-dependent activation are apparently uncoupled. This result by itself indicates that D102 is involved in the propagation of NO activation following the H105−iron breakage and is indirectly supported by our finding that D102N is not activated by PPIX, an iron-free heme activator. We ruled out that the observed uncoupling is due to drastically decreased heme content in D102N as the characteristics of purification of WT and D102N are similar, as is the A280/A431 ratio, and the Soret shift from 431 to 398 nm upon addition of NO. Our structural modeling predicts that D102 interacts with the backbone of F120 and with H105 via a molecule of water but is also solvent-exposed favoring interaction with another part of the enzyme, probably the catalytic domain of sGC, a potential key step in the propagation of NO activation.[12] Moreover, D102 is part of the αF helix that is known to undergo a large shift upon NO binding and H105−iron bond breakage. We speculate that the mutation D102N while allowing the formation of the nitrosyl−heme upon NO binding, would alter the interaction with the cyclase domain (or another domain) as follows: the oxygen atom in N102 still makes the interaction with the backbone nitrogen of F120 (thus maintaining the integrity of this heme region in the 5c NO-bound state) but the free solvent exposed oxygen in D102 is now a

nitrogen in N102, thus potentially disrupting interaction with another domain. This "dichotomy" of functions of D102, e.g., involvement in the structural interactions of this heme domain region and transduction of the NO signal via the triad H105−water−D102 might be the reason for its invariability in known sGC sequences (as otherwise an asparagine at this position would have sufficed). Another potential explanation for the D102N uncoupling phenotype is that D102 interacts with H105 *only* when it is released from the heme iron. However, molecular dynamic simulation (not shown) and our recent structural data of the *Nostoc* HNOX activated state with Bay 58−2667[22] show no clear evidence of such transition.

Incidentally, activation by YC-1 of D102N is marginal but combination of YC-1 and NO leads to significant increase in the mutant activity. Because YC-1 increases affinity of NO for the heme, one possible explanation was that the heme of D102N has a decreased affinity for NO. However, DEA-NO concentration response curves indicate that affinity of the heme for NO did not seem to be involved as specific activity does not increase as a function of increasing concentrations of NO in the range of 1−100 μM. Yet in the presence of YC-1, the specific activity is greatly increased in this same range of NO (from 1 to 100 μM). Taken together these results suggest that, in this mutant, YC-1 potentiates the NO effect by additional means such as increased NO efficacy, as we previously suggested.[23] We can propose two mechanisms to explain that the heme-nitrosyl still forms in D102N and that increased NO concentration does not lead to increased activity except in the presence of YC-1: (a) there are two distinct but not mutually exclusive conformational changes that take place upon NO binding and downstream of the His−iron bond cleavage; one can increase catalysis in the absence of YC-1 while the other one increases catalytic activity only when YC-1 is bound to sGC. The mutation D102N by disrupting the former conformational change unmasks the latter. (b) NO binds to a non-heme site to activate sGC independently of the heme−nitrosyl formation. This will explain that YC-1 can increase NO efficacy independently of NO affinity; indeed, using butyl isocyanide to occupy sGC heme, it was found that NO could still increase sGC activity without formation of the nitrosyl−heme complex and that YC-1 had a synergistic effect under these conditions.[24] It was later determined, using thiol blocking reagents, that binding of NO to a cysteine of sGC was potentially the independent heme−nitrosyl mechanism of activation.[25]

In summary, our structure-based mutational analysis of the HNOX domain in full-length sGC indicates the crucial role of D102 for NO activation. Further experiments will be needed to assess whether D102 is involved in direct interaction with another domain and the mechanism of synergistic activation of YC-1.

■ ASSOCIATED CONTENT

Supporting Information. Tables 2 and 3 and Figures 1−3. This material is available free of charge via the Internet at http://pubs.acs.org.

■ AUTHOR INFORMATION

Corresponding Author

*E-mail focco.vandenakker@case.edu, Ph (216) 368-8511 (F.v.d.A.); e-mail annie.beuve@umdnj.edu, Ph (973) 972 8838, Fax 973-972-4554 (A.B.).

Funding Sources

This work was supported by National Institutes of Health Grants GM067640 (to A.B.) and HL075329 (to F.v.d.A).

■ ABBREVIATIONS

H-NOX, heme nitric oxide and oxygen; sGC, soluble guanylyl cyclase; NO, nitric oxide; WT, wild-type; SNAP, *S*-nitroso-*N*-acetyl-penicillamine; DEA-NO, 2-(*N*,*N*-diethylamino)diazenolate-2-oxide; YC-1, 5-[1-(phenylmethyl)-1*H*-indazol-3-yl]-2-furanmethanol.

■ REFERENCES

(1) Ignarro, L. J., Cirino, G., Casini, A., and Napoli, C. (1999) Nitric oxide as a signaling molecule in the vascular system: an overview. *J. Cardiovasc. Pharmacol. 34*, 879–886.

(2) Moncada, S., Palmer, R. M., and Higgs, E. A. (1991) Nitric oxide: physiology, pathophysiology, and pharmacology. *Pharmacol Rev 43*, 109–142.

(3) Snyder, S. H., and Bredt, D. S. (1991) Nitric oxide as a neuronal messenger. *Trends Pharmacol. Sci. 12*, 125–128.

(4) Wedel, B., Humbert, P., Harteneck, C., Foerster, J., Malkewitz, J., Bohme, E., Schultz, G., and Koesling, D. (1994) Mutation of His-105 in the beta 1 subunit yields a nitric oxide- insensitive form of soluble guanylyl cyclase. *Proc. Natl. Acad. Sci. U.S.A. 91*, 2592–2596.

(5) Nioche, P., Berka, V., Vipond, J., Minton, N., Tsai, A. L., and Raman, C. S. (2004) Femtomolar sensitivity of a NO sensor from Clostridium botulinum. *Science 306*, 1550–1553.

(6) Pellicena, P., Karow, D. S., Boon, E. M., Marletta, M. A., and Kuriyan, J. (2004) Crystal structure of an oxygen-binding heme domain related to soluble guanylate cyclases. *Proc. Natl. Acad. Sci. U.S.A. 101*, 12854–12859.

(7) Ma, X., Sayed, N., Beuve, A., and van den Akker, F. (2007) NO and CO differentially activate soluble guanylyl cyclase via a heme pivot-bend mechanism. *EMBO J. 26*, 578–588.

(8) Capece, L., Estrin, D. A., and Marti, M. A. (2008) Dynamical characterization of the heme NO oxygen binding (HNOX) domain. Insight into soluble guanylate cyclase allosteric transition. *Biochemistry 47*, 9416–9427.

(9) Schmidt, P. M., Schramm, M., Schroder, H., Wunder, F., and Stasch, J. P. (2004) Identification of residues crucially involved in the binding of the heme moiety of soluble guanylate cyclase. *J. Biol. Chem. 279*, 3025–3032.

(10) Schmidt, P. M., Rothkegel, C., Wunder, F., Schroder, H., and Stasch, J. P. (2005) Residues stabilizing the heme moiety of the nitric oxide sensor soluble guanylate cyclase. *Eur. J. Pharmacol. 513*, 67–74.

(11) Martin, E., Sharina, I., Kots, A., and Murad, F. (2003) A constitutively activated mutant of human soluble guanylyl cyclase (sGC): implication for the mechanism of sGC activation. *Proc. Natl. Acad. Sci. U.S.A. 100*, 9208–9213.

(12) Winger, J. A., and Marletta, M. A. (2005) Expression and characterization of the catalytic domains of soluble guanylate cyclase: interaction with the heme domain. *Biochemistry 44*, 4083–4090.

(13) Martin, F., Baskaran, P., Ma, X., Dunten, P. W., Schaefer, M., Stasch, J. P., Beuve, A., and van den Akker, F. (2010) Structure of cinaciguat (BAY 58−2667) bound to Nostoc H-NOX domain reveals insights into heme-mimetic activation of the soluble guanylyl cyclase. *J. Biol. Chem. 285*, 22651–22657.

(14) Olea, C., Jr., Herzik, M. A., Jr., Kuriyan, J., and Marletta, M. A. (2010) Structural insights into the molecular mechanism of H-NOX activation. *Protein Sci. 19*, 881–887.

(15) Erbil, W. K., Price, M. S., Wemmer, D. E., and Marletta, M. A. (2009) A structural basis for H-NOX signaling in Shewanella oneidensis by trapping a histidine kinase inhibitory conformation. *Proc. Natl. Acad. Sci. U.S.A. 106*, 19753–19760.

(16) Arnold, K., Bordoli, L., Kopp, J., and Schwede, T. (2006) The SWISS-MODEL workspace: a web-based environment for protein structure homology modelling. *Bioinformatics 22*, 195–201.

(17) Yuen, P. S., Doolittle, L. K., and Garbers, D. L. (1994) Dominant negative mutants of nitric oxide-sensitive guanylyl cyclase. *J. Biol. Chem. 269*, 791–793.

(18) Chang, F. J., Lemme, S., Sun, Q., Sunahara, R. K., and Beuve, A. (2005) Nitric oxide-dependent allosteric inhibitory role of a second nucleotide binding site in soluble guanylyl cyclase. *J. Biol. Chem. 280*, 11513–11519.

(19) Ignarro, L. J., Wood, K. S., and Wolin, M. S. (1982) Activation of purified soluble guanylate cyclase by protoporphyrin IX. *Proc. Natl. Acad. Sci. U.S.A. 79*, 2870–2873.

(20) Friebe, A., and Koesling, D. (1998) Mechanism of YC-1-induced activation of soluble guanylyl cyclase. *Mol. Pharmacol. 53*, 123–127.

(21) Olea, C., Boon, E. M., Pellicena, P., Kuriyan, J., and Marletta, M. A. (2008) Probing the function of heme distortion in the H-NOX family. *ACS Chem. Biol. 3*, 703–710.

(22) Martin, F., Baskaran, P., Ma, X., Dunten, P. W., Schaefer, M., Stasch, J. P., Beuve, A., and van den Akker, F. (2010) Structure of cinaciguat (bay 58−2667) bound to nostoc H-NOX domain reveals insights into heme-mimetic activation of the soluble guanylyl cyclase. *J. Biol. Chem.*

(23) Lamothe, M., Chang, F. J., Balashova, N., Shirokov, R., and Beuve, A. (2004) Functional Characterization of Nitric Oxide and YC-1 Activation of Soluble Guanylyl Cyclase: Structural Implication for the YC-1 Binding Site? *Biochemistry 43*, 3039–3048.

(24) Derbyshire, E. R., and Marletta, M. A. (2007) Butyl isocyanide as a probe of the activation mechanism of soluble guanylate cyclase. Investigating the role of non-heme nitric oxide. *J. Biol. Chem. 282*, 35741–35748.

(25) Fernhoff, N. B., Derbyshire, E. R., and Marletta, M. A. (2009) A nitric oxide/cysteine interaction mediates the activation of soluble guanylate cyclase. *Proc. Natl. Acad. Sci. U.S.A. 106*, 21602–21607.